Nanoscale Properties of Poly(ethylene terephthalate) Vascular Grafts

By

Celia Edith Macias

Submitted to the Department of Materials Science and Engineering
in Partial Fulfillment of the Requirements for the Degree of

Bachelor of Science

at the

Massachusetts Institute of Technology

June 2004

© 2004 Celia Edith Macias
All Rights Reserved

Signature of Author ....
Department of Materials Science and Engineering
May 7, 2004

Certified by ....
Prof. Christine Ortiz
Assistant Professor of Materials Science and Engineering
Thesis Supervisor

Accepted by ....
Prof. Lorna Gibson
Professor of Materials Science and Engineering
Chairman, Undergraduate Thesis Committee

Nanoscale Properties of Poly(ethylene terephthalate) Vascular Grafts

By

Celia Edith Macias

ABSTRACT

Vascular grafts are prosthetic tubes that serve as artificial replacements for damaged blood vessels. Poly(ethylene-terephthalate), PET, has been successfully used in large diameter grafts; however, small caliber grafts are still a major challenge in biomaterials. Due to surface forces, blood plasma proteins adsorb to the graft, resulting in inflammation, infection, thrombus formation, and ultimately, vessel reclosure. The object of this project was to characterize and analyze the nanoscale surface properties of three different commercial vascular grafts, woven collagen-coated, knitted collagen-coated, and knitted heparin-bonded, all PET-based. The study was performed in order to ascertain differences in biocompatibility due to surface coating and morphology. Scanning Electron Microscopy, Atomic Force Microscopy and High Resolution Force Spectroscopy techniques were used to characterize the surface of the samples as well as to measure the forces between these surfaces and blood plasma proteins. The results will serve as a basis for the understanding of the nanoscale interactions between the biomaterial and blood plasma proteins. Such interactions are brought about by the different surface topologies and components, therefore a thorough understanding of surface properties will act as a building block for further changes in small caliber vascular grafts in order to enhance their biocompatibility.

TABLE OF CONTENTS

LIST OF TABLES, FIGURES, AND IMAGES

ACKNOWLEDGEMENTS

CHAPTER 1
INTRODUCTION AND BACKGROUND

1.1. BIOMATERIALS AND BIOCOMPATIBILITY

A biomaterial is a synthetic material used to replace part of a living system or to function in intimate contact with living tissue. Biomaterials are said to be biocompatible if they are able to perform a specific function in biological conditions without causing an undesired response from the host's immune system [1].

A major challenge existing in the field of blood-contacting biomaterials is the prevention of nonspecific, noncovalent surface adsorption of proteins [2]. While protein adsorption can be desirable for certain applications, such as tissue engineering and bone implant, it should be avoided in vascular grafts. Blood proteins adsorb to an arterial prosthesis (Figure 1.1) upon blood flow exposure, triggering the activation of platelet formation, eventually resulting in thrombus formation and vessel reclosure [3].
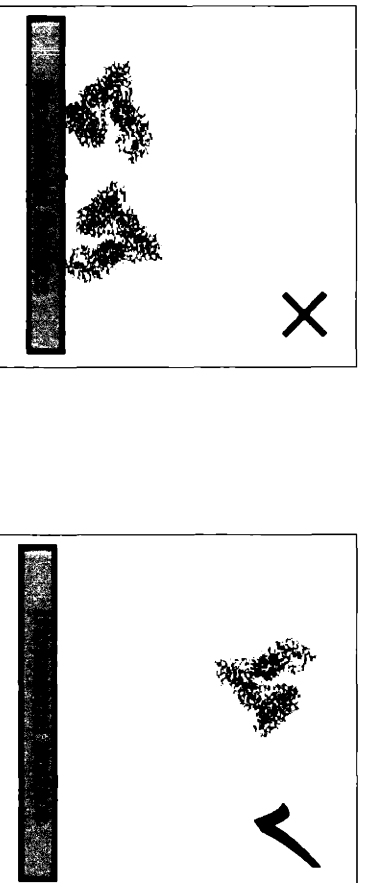
Figure 1.1. LEFT: Adsorption of blood plasma proteins onto biomaterial surface: undesirable reaction. RIGHT: Proteins do not adsorb to surface of biocompatible materials.

The interaction potential energy, U, as a function of the protein-surface separation distance, D, $U(D) = -\int F(D)dD$ will determine whether or not a protein will initially adsorb to a biomaterial surface. The net interaction is a superposition of numerous nonspecific repulsive interactions such as electrostatic counterion double layer, steric, hydration, etc., as well as attractive interactions such as van der Waals, hydrophobic, H-bonding, ionic, etc. The adsorption process of proteins onto the surface of biomaterials is determined by the total interaction free energy between the protein and the material surface. According to this relationship, an ideal engineered biomaterial surface minimizes attractive and maximizes repulsive interactions. However, this relationship does not necessarily dictate the fate of the biomaterial in the human body. According to the Vroman effect [4], low molecular weight molecules govern the protein-polymer interactions in the early stages of protein adhesion. This process is overtaken at later stages by molecules with higher surface affinities. Therefore, secondary stages, protein adsorption depends on biomolecular adhesive binding processes that take place when the protein is in close contact with the surface, the conformation, orientation, and mobility of the adsorbed proteins, the time scale of conformational changes, protein exchange and desorption, and interactions of adsorbed proteins with each other. Nonetheless, an understanding of the first stage of protein adsorption provides a foundation to determine the biocompatibility of materials.

1.2. VASCULAR GRAFTS

The most common cardiovascular disease, atherosclerosis, reduces the caliber of arteries, hindering blood flow. This situation leads to surgery in order to replace damaged arteries [3, 5]. Vascular grafts are prosthetic tubes that serve as artificial replacements for damaged blood vessels [6]. Synthetic, textile vascular grafts have been successfully used in large diameter grafts; however, small caliber grafts are still a major challenge in biomaterials.

A vascular graft should meet the following properties: 1) desirable biocompatibility, 2) viscoelastic properties similar to blood vessels so that it is sufficiently compliant but will not allow for overexpansion or bursting, 3) long-term mechanical stability, 4) prevent graft leakage which can lead to seroma formation and blood loss, and 5) be abrasion resistant. Presumably, biomaterial surfaces will be more compatible with the human body if they have similar chemistry, morphology and mechanical properties to cell surfaces.
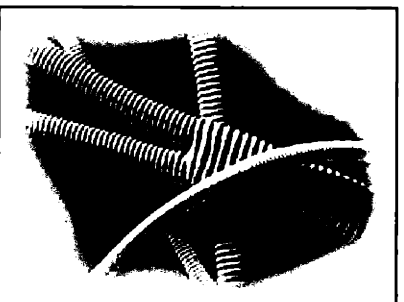
Figure 1.2. Commercial vascular graft [*http://www.intervascular.com/us/*]

Due to surface forces, blood plasma proteins adsorb to the graft, resulting in inflammation, infection, thrombus formation, and ultimately, vessel reclosure. To prevent thrombus formation, grafts are sometimes bonded with heparin, an anticoagulant drug. While this method yielded satisfactory results in clinical trials, the design of small caliber grafts with successfully protein-resistant surfaces are still a major challenge for biomaterials scientists [3] because a clot is more likely to obstruct blood flow in a narrow conduit than in a wide one.

A very commonly used material for vascular grafts is poly(ethylene terephthalate) also known as PET or Dacron®. PET has been successfully used in large diameter grafts. Small caliber grafts still show an unsatisfactorily high percentage of failure *in vivo* [5].

1.3. COMMERCIAL SAMPLES

Four different types of vascular grafts were studied (Intervascular®, Montale, NJ): *1)* a non-commercial woven PET sample (used as a control), and the commercially available *2)* woven collagen-coated PET (IGW0038-30), *3)* knitted collagen-coated PET sample (IGK0006-40), and *4)* knitted PET sample bound with collagen and heparin (IGK0006-40H). The vascular grafts provided are soft, macroscopically crimped cylindrical conduits, sterilized by Gamma irradiation. Following is a description of all the nonproprietary information provided by the manufacturer. The dimensions, physical, and mechanical properties of the grafts are given in Table 1.1.

Table 1.1 Dimensions, physical and mechanical properties of commercial vascular grafts used in this study (Intervascular®).

Sample	Fabric Construction	Water Permeability	Wall thickness/Length	Burst Strength	45 degree suture retention
1	Bare Polyester Untreated polyester	Not provided	0.38 mm	Not provided	Not provided
2	Woven (Collagen Coated) Cross-linked Type 1 bovine collagen	$\leq$ 5ml • cm^{-2} • min^{-1} @120 mmHg	0.38 mm	Not provided	2.53 kg
3	Knitted (Collagen Coated) Cross-linked Type 1 bovine collagen Knitted, external velour, reverse locknit	$\leq$ 5ml • cm^{-2} • min^{-1} @120 mmHg	0.49 mm	32.7 kg/cm^2	3.37 kg
4	Knitted (Heparin bonded) Cross-linked Type 1 bovine collagen Knitted, external velour, reverse locknit	$\leq$ 5ml • cm^{-2} • min^{-1} @120 mmHg	0.49 mm	32.7 kg/cm^2	3.37 kg

The graft's crimps are obtained by heat treatment, which (according to the manufacturer), does not degrade the integrity of the polyester fibers [7]. Two different types of interweaved grafts were studied: woven and knitted (Figure 1.3).
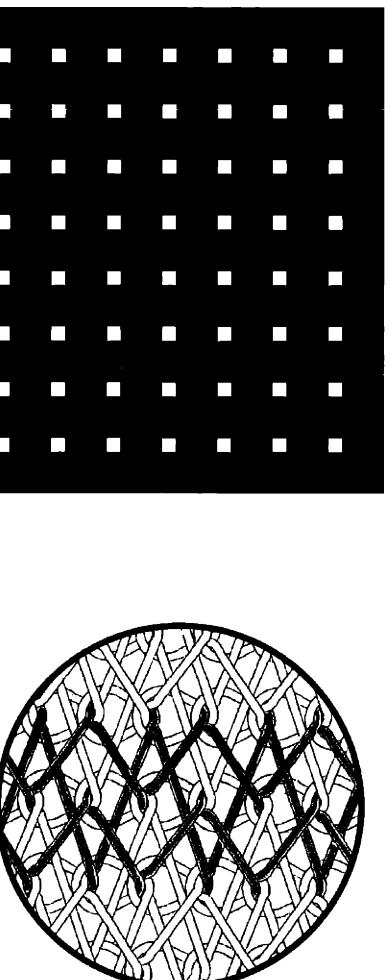
Figure 1.3. LEFT: Representation of woven fiber bundles. RIGHT: knitted, reverse locknitted fiber bundles [http://www.intervascular.com] used for PET vascular grafts.

The woven structure consists of a regular interlocking of fiber bundles, as shown in Figure 1.3 (left). These grafts (bare PET and collagen) are less stiff than the knitted ones and are expected to have higher porosity. The knitted grafts (collagen and heparin) are stiffer than the woven ones, due to their more complicated knitting: InterGard's proprietary knit design called Reverse Locknit, as seen in Figure 1.3 (right). Knitted grafts are often preferred by surgeons because they exhibit minimal fiber unraveling upon suturing [8].

In addition the differences in fiber structure, the graft samples also differ in surface chemistry. The bare PET sample was left untreated and it is clean and unmodified. Both woven and knitted collagen-coated grafts were treated to seal the pores in the grafts using Intergard's proprietary coating process. The heparin bonded graft contains a gradient of heparin concentration, with the highest concentration being near the inside wall of the graft as seen in Figure 1.4.
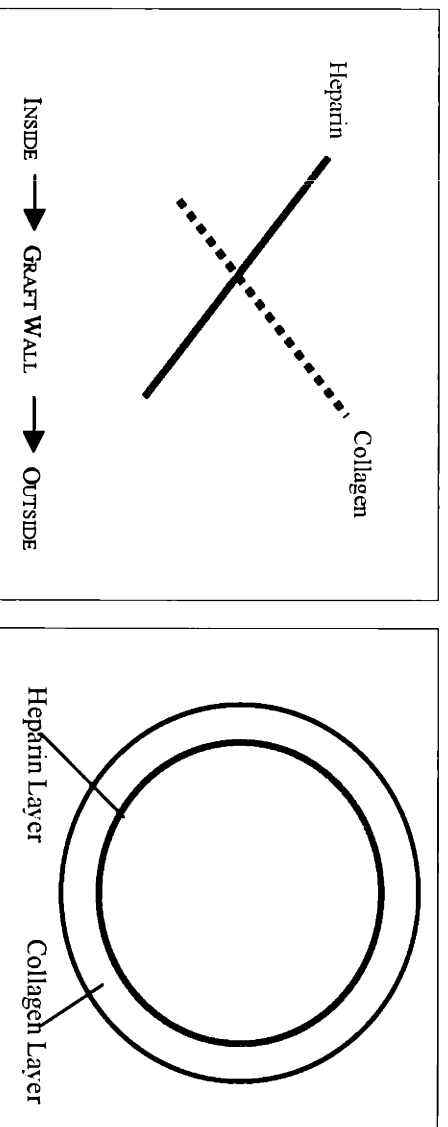
Figure 1.4. LEFT: Distribution of Heparin and Collagen: across the graft wall. RIGHT: graft cross section

1.4. POLY(ETHYLENE TEREPHTHALATE)

Poly(ethylene terephthalate), PET, is the most common of the polyesters. PET has a melting temperature of about 265°C and at room temperature it is resistant to most of the common organic solvents as well as humidity [9].

PET is polymerized from ethylene glycol and terephthalic acid monomers. The first step is the esterification of the acid with ethylene glycol. This is followed by polycondensation and removal of the ethylene glycol byproducts. The result is a clear, glassy solid, with aromatic rings hindering the mobility of the polymer chain [10]. PET's chemical structure is shown in Figure 1.5. Its glass transition temperature is around 70°C [10].

Figure 1.5. Chemical structure of polyethylene terephthalate [11]

Usually, PET is extruded through small holes at slow speeds to form fibers. The resulting fibers are then stretched, aligning the polymer molecules in the direction of stretching. Finished PET fibers are semicrystalline (~50% crystallinity). PET fibers usually contain from 0.03 to 0.4 weight percent of titanium dioxide (used as a delustering agent). This additive possibly affects the surface topology of the polyester fibers [10].

Currently, PET is the preferred polymer for medium and large caliber vascular grafts, because of the wide variety of types, linear densities, filament counts, filament

diameters, cross-sectional shapes and textured modifications that can be achieved during the manufacturing process [12].

PET is known to prevent vascular healing and it is considered to be inflammatory and thrombogenic, presumably due to its hydrophobic nature [6] (contact angle ~70 degrees [13]); however, its ease of needle penetration, handling characteristics, desirable mechanical and physical properties, and chemical stability make it an attractive candidate for vascular grafts [6]. Therefore, the surface of polyester vascular grafts is modified in order to improve their biocompatibility while preserving PET's bulk characteristics.

Another major challenge encountered in the early years of vascular graft use was the leaking of blood through the graft's pores. This issue was first addressed by pre-clotting the graft using the patient's own blood prior to surgery. The pre-clotting method showed to be inconvenient as well as dangerous [25]. The next generation of synthetic vascular grafts was designed to prevent leakage by adding a collagen coat to the surface of the graft, which acts as a sealant.

1.5. COLLAGEN

Collagen is a fibrous protein that occurs in almost all mammalian tissues. The amino acid sequence of collagen consists of –Gly-Pro-Hyp-Gly-X- where X could be any amino acid [14]. Table 1.2 shows the amino acid content of collagen. Collagen has an isoelectric point (pH at which the total charge is zero) of around 4.5 [15] and a contour length of 309±41 nm [16].

Table 1.2. Amino acid content of collagen [14]

Amino acids	Mol/100 mol amino
Gly	31.4-338
Pro	11.7-13.8
Hyp	9.4-10.2
Acid polar (Asp, Glu, Asn)	11.5-12.5
Basic polar (Lys, Arg, His)	8.5-8.9
Other	Residue

Collagen is added to vascular grafts to replace the need for pre-clotting (used to 'seal' porous grafts). It also acts as a temporary scaffold to promote cell growth and graft healing. *The collagen coat used for the grafts studied here is cross-linked Type I bovine.*

On the other hand, collagen is highly thrombogenic and it is an activator of the blood-clotting cascade [17], undesirable characteristics of a vascular graft surface. A current method used to reduce the thrombogenicity of collagen-coated, small diameter vascular grafts is to attach heparin –an anticoagulant drug- to the surface.

1.6. THROMBOSIS

A blood clot, also known as thrombus, is a common problem observed in blood-contacting devices such as vascular grafts. Plasma proteins adsorb onto the surface of the vascular graft, activating platelet adhesion and triggering the coagulation cascade [5] ultimately resulting in thrombus formation and vessel reclosure. Low molecular weight molecules, such as human serum albumin govern the protein-polymer interactions

in the early stages of protein adhesion. This process is overtaken at later stages by molecules with higher surface affinities as predicted by the Vroman Effect [4].

Platelet adhesion on vascular grafts is determined by their surface area, texture, and chemistry, charge, and topography [5,6,18]. A smooth surface results in a small surface area, reducing platelet adhesion. However, commercial vascular grafts show a high degree of porosity, increasing the surface area available for protein adhesion.

An approach currently used in biomaterials to inhibit thrombus formation is the immobilization of an anticoagulant drug, heparin, onto the surface of the material.

1.7. HEPARIN

Heparin is the most biologically reactive member of the family of sulfated glycosaminoglycans (GAGs), which are widespread in animal tissue [19] and it is the most widely used drug to modify the surfaces of vascular implants [18,20]. Its chemical structure is shown in Figure 1.6.
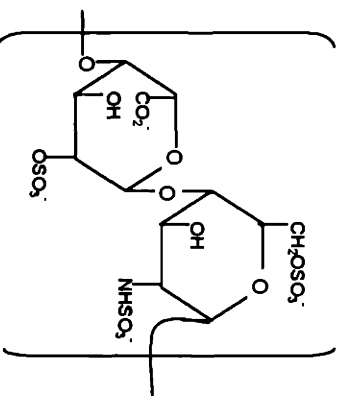
Figure 1.6. Chemical structure of Heparin [19]

15

Heparin is a negatively charged polysaccharide that possesses antithrombotic and anticoagulant properties by increasing the activity of antithrombin III (an inhibitor of the coagulation cascade) [21]. It achieves this by binding to either plasma heparin cofactor II or antithrombin, catalyzing their inhibition of thrombin and other coagulation factors.

Heparin is coupled to the surface of PET-based commercial vascular grafts using *tri-dodecylammonium chloride (TDMAC)* which forms an insoluble complex with heparin and binds with high affinity to the polyester flow surface through its long hydrophobic tails [7]. The chemical structure of TDMAC is shown in Figure 1.7. Heparin will bind ionically (noncovalently) to the positively charged nitrogen of the TDMAC.

$$CH_3-(CH_2)_{11}$$
$$CH_3-(CH_2)_{11}-N^+-CH_3$$
$$CH_3-(CH_2)_{11}$$
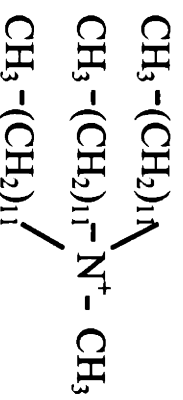
Figure 1.7. Chemical Structure of tri-dodecylammonium chloride (TDMAC) [7]

The heparinized graft is also coated with collagen which acts as a barrier to prevent rapid release of the heparin from the graft surface [7], and also prevents blood leakage.

CHAPTER 2
EXPERIMENTAL METHODS

2.1. *SURFACE MORPHOLOGY AND CHARACTERIZATION*

Surface morphology plays a very important role in the immunological rejection response caused by the implantation of a synthetic biomaterial in the human body. Platelet adhesion on vascular grafts is partially determined by surface area, texture, and topography. Smooth surfaces exhibit small surface areas, reducing platelet adhesion. A thorough understanding of surface topography, complemented by high resolution force spectroscopy studies will reveal the dependence of protein adhesion on biomaterials surface properties.

2.1.1. SCANNING ELECTRON MICROSCOPY

Graft samples were analyzed using the Scanning Electron Microscope (JOEL JSM-5910) under 10eV voltage. Scanning Electron Microscopy (SEM) samples are placed inside an air-tight chamber. Under vacuum, an electron gun emits a beam of high energy electrons, which travels toward the sample through a series of magnetic lenses which focus the electrons. The focused beam of electrons scans across the sample. As the electron beam hits the sample, secondary electrons are released from its surface. A

detector counts these electrons and emits a signal. SEM images are produced from the count of electrons emitted from the sample.

Samples were prepared by cutting 1cm² pieces from the different grafts using clean scissors. The pieces were then placed on a sample holder. The sample holder used features two spring clips to hold the sample down without the need to glue the sample down. Colloidal Graphite (Ted Pella, #16053) was used to bridge the conductivity from the clips to the sample. The samples were then coated with gold and stored in an airtight, sealed container prior to and immediately after imaging.

2.1.2. ATOMIC FORCE MICROSCOPY

The NanoScope IIIA Multimode™ Atomic Force Microscope (Veeco Metrology, Digital Instruments), henceforth referred to as the AFM is a tool widely used in the imaging field. The AFM system consists mainly of a piezoelectric scanner, a cantilever probe tip, a photodiode detector and a computer (Figure 2.1). The computer controls the system and performs data acquisition, display and analysis. The piezoelectric scanner positions the sample with Angstrom accuracy. The cantilever probe tip senses surface properties, causing it to deflect as the sample surface is scanned. The cantilever deflection is measured by the photodiode by means of a laser diode reflected off the back of the cantilever. The computer then analyzes the data and converts it to an image.

18

laser diode

mirror

sensor output, δc, Fc

cantilever
· spring which deflects as probe tip scans sample surface

position sensitive photodetector
· measures deflection of cantilever

| A | B |
| C | D |

probe tip
· senses surface properties and causes cantilever to deflect

computer
· controls system
· performs data acquisition, display, and analysis

≈10°-15°

δc

sample

piezoelectric scanner
· positions sample (x, y, z) with Å accuracy

z y x

feedback loop
· controls z-sample position

ERROR = actual signal - set point

Figure 2.1. Atomic Force Microscope schematic.

Samples were prepared by cutting 1cm^2 pieces from the different grafts using clean scissors. The pieces were either mounted on a especially designed sample holder or glued to a magnetic sample holder using a thin layer of adhesive (much thinner than the graft thickness), pressed against freshly cleaved mica, and left to dry under a 5 kg weight to release the wrinkles in order to allow for tip-surface engagement. The samples were stored in an airtight, sealed container prior to and immediately after imaging.

AFM images of the vascular graft samples were taken under different conditions to determine the effect of sample preparation. All images were taken in air under contact mode.

2.2. PROTEIN-GRAFT INTERACTIONS

High Resolution Force Spectroscopy experiments were conducted using the 1-D Molecular Force Probe (MFP) in order to measure force, F (nN), versus tip-sample separation distance, D (nm). The results obtained will be compared to the surface morphology results and will serve as a basis for the understanding of the nanoscale interactions between the biomaterial and blood plasma proteins.

2.2.1. MOLECULAR FORCE PROBE

The molecular interactions with blood proteins will be studied using a single axis force tracer, the *Molecular Force Probe (Asylum Research, Santa Barbara CA)*, henceforth referred to as the MFP. In a manner similar to the AFM, the MFP measures forces between a probe tip and a surface (limits of detection: force $\geq \pm 5$ pN, displacement $\geq \pm 3$ Å) by means of a system comprised of a laser diode, a cantilever probe tip, a piezoelectric scanner, a photodiode and a computer. The piezoelectric moves the tip towards ("approach") and away from the sample ("retract") at a constant rate, while the photodiode measures the reflection of the cantilever probe tip. The computer then analyzes the data, converting it to force versus distance curves. Blood proteins were covalently attached to a cantilever probe tip and the forces between the tip and the vascular graft sample were measured and analyzed.

Figure 2.2. Molecular Force Probe schematic
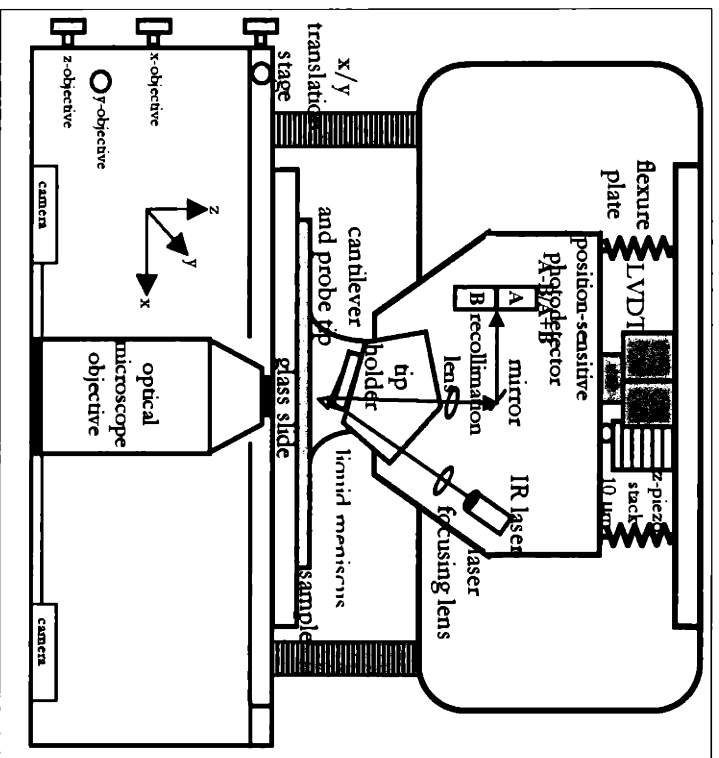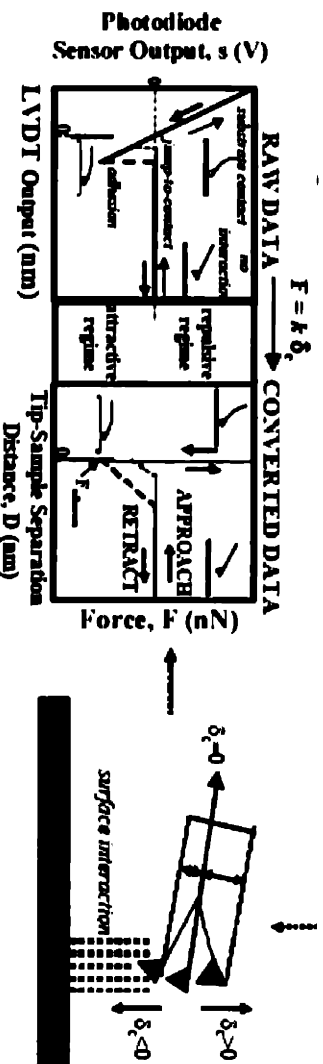

Figure 2.3. LEFT: Typical HRFS force versus distance curve. RIGHT: Deflection of a cantilever in response to intermolecular interactions with the surface

Force versus distance curves were measured at room temperature using a Thermomicroscopes microfabricated V-shaped Si_3N_4 cantilever probe tip ($k_c = 0.01$ N/m, cantilever length = 320 μm, resonant frequency = 850 Hz).

Figure 2.4. Microfabricated cantilever probe tip used in MFP experiments

2.2.1.A. TIP FUNCIONALIZATION

Blood plasma contains thousands of different types of proteins. In order to simplify nanoscale protein adsorption studies, a model protein, human serum albumin (HSA) was chosen.

Human serum albumin is a highly water-soluble plasma protein. It is the smallest and most abundant plasma protein in the human body, accounting for 55% of the protein content in blood plasma [22]. Because of its low molecular weight, it is one of the first to adsorb to a blood-contacting implanted biomaterial [4]. Due to this property, HSA was chosen over antithrombin (which is known to bind specifically to heparin, a drug contained in one of the samples studied). The results will then show only the nonspecific interactions between HSA and the graft samples.

HSA is a single-stranded polypeptide. Its ionizable groups include 98 carboxyl, 18 phenolic —OH, 60 amino, 16 imidazolyl, 24 guanidyl [22]. The absolute molecular weight of HSA is 66,436 g/mol (calculated from the molar masses of the 565 constituent

amino acids). The total contour length of the denatured protein is $L_{contour}(HSA) = 216$ nm (assuming a polypeptide repeat unit contour length of 0.38 nm).

Using the technique of High Resolution Force Spectroscopy, the nanoscale interactions between human serum albumin and the surface of commercial vascular grafts will be measured.

The square pyramidal probe tip found at the end of the cantilevers was chemically modified with HSA using the chemical reaction scheme [23] shown in Figure 2.5.
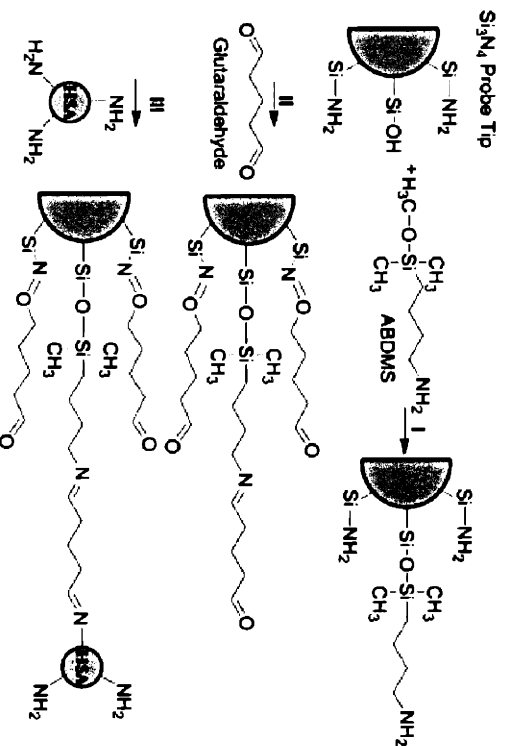
Figure 2.5. Chemical reaction scheme for the covalent attachment of HSA to a Silicon Nitride cantilever probe tip [23].

Aminobutyldimethylmethoxysilane (ABDMS, #S565350), glutaraldehyde (#G-8552, lot #31K5306), and HSA (#A9511, lot#126H9322) were purchased from Sigma. Si$_3$N$_4$ probe tips were cleaned and oxidized in oxygen plasma for 10 seconds at 30 Pa and 10 W power immediately preceding modification. They were then immersed in a 4% (v/v) toluene solution of ABDMS for 2 hours, and then rinsed in methanol followed by 0.01 M PBS (Phosphate Buffer Solution) before being immersed in a 2.5% (v/v) aqueous solution of glutaraldehyde for 30 minutes and then rinsed with copious amounts of deionized (DI) water. The tips were then incubated for 60 seconds in a 0.01% (w/v) HSA

solution in 0.01M PBS, then rinsed with and stored in 0.01M PBS. The ABDMS and glutaraldehyde molecules provide a short linker for the HSA off the probe tip, allowing for some flexibility and retention of the native movements of the protein.

Following the experimental setup described in Figure 2.6, the net nanoscale forces as a function of the separation distance between HSA and the different vascular grafts were measured using the MFP.
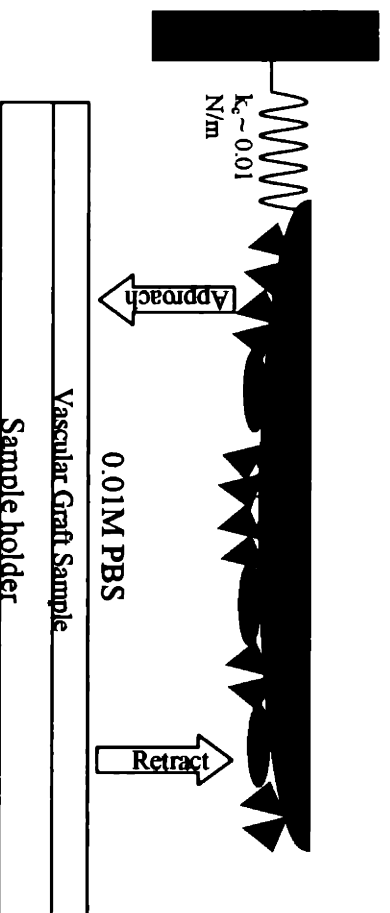
Figure 2.6. Experimental setup for MFP experiments

2.2.2. *DATA AND STATISTICAL ANALYSIS*

Force versus distance curves on approach from three different sites on the sample surface were averaged and the standard deviations were calculated. For retract curves, the data was not averaged because of the large adhesion force and distance distributions inherent in the nonspecific adhesion. Instead, statistical analysis of the maximum forces and distances of adhesion under each of the experimental conditions was performed. Figure 2.7 shows typical force versus distance curves for the different events observed in high resolution force spectroscopy experiments on retract. Non-adhesive events (bottom

left) show continuous approach and retract curves. Protein adhesion events (bottom center) show cantilever instability regions after the protein extension. Surface adhesion events (bottom right) are characterized by pulls at small distances followed by cantilever stability regions. In order to analyze the retract data, the force and distance coordinate of the bottom-most point in protein extension and surface adhesion curves were recorded and averaged.
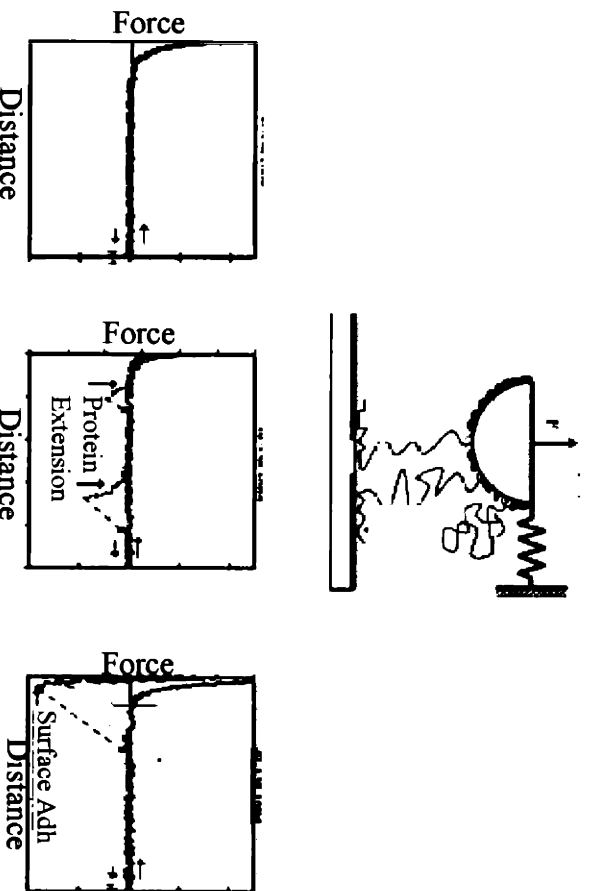
Figure 2.7. Typical protein-surface interaction profiles. TOP: Schematic of protein extension. BOTTOM LEFT: Typical non-adhesive force vs. distance curve. BOTTOM CENTER: Typical force vs. distance curve exhibiting protein extension. BOTTOM RIGHT: Typical force vs. distance curve exhibiting surface adhesion.

Significance of the statistical analysis was calculated using student's 'τ' test (Graph Pad InStat, GraphPad Software, San Diego, CA). Results were considered statistically different with p<0.05.

25

CHAPTER 3
RESULTS AND DISCUSSION

3.1. SURFACE ANALYSIS

3.1.1. SCANNING ELECTRON MICROSCOPY

The Scanning Electron Microscope images obtained from the vascular grafts revealed the surface morphology expected from the schematics in Figure 1.3. Image 3.1 shows the inside (blood-contacting) wall of the woven collagen-coated sample. The average fiber bundle width is 250 ± 38 μm ($n=15$), and the average crimp width is 1180 ± 105 μm ($n=6$). It should be noted that the bubble-like features located between crimps (average diameter= 620 ± 493 μm, $n=10$) are believed to be the degrading collagen film (due to sample damaging caused by applied voltage).
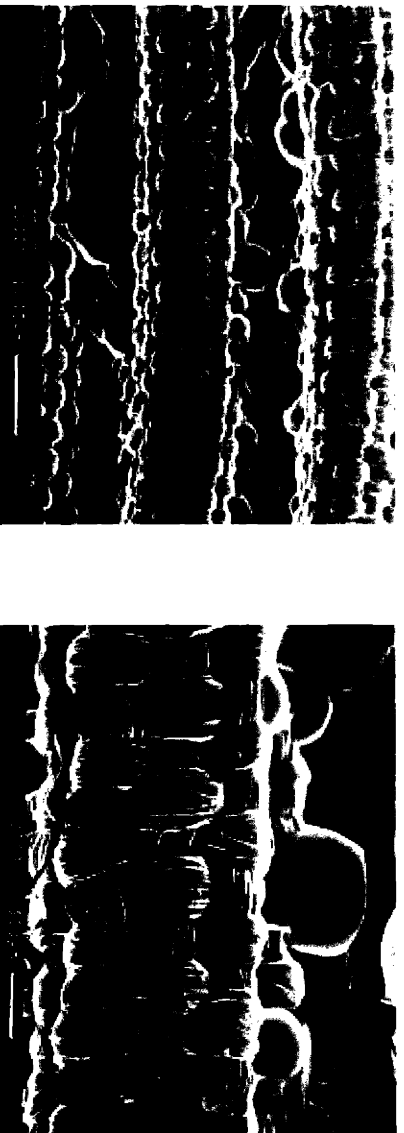
Image 3.1. SEM images of PET vascular graft, inside wall (Woven, collagen-coated)

Image 3.2, both left and right, shows SEM images of fibers found in the same sample used above. The left image agrees with the reasonable PET fiber diameter [18] of

26

20 ± 5 μm (n=10). The right image shows a fiber bundle. This fiber bundle consists of 55 fibers. The image shows the non-circular geometry of the PET fibers, probably caused by the stretching of the fiber bundles after the extrusion process. This feature could potentially be undesirable, as it does not possess the 'smoothness' of a circular fiber (See section 1.7).

Image 3.2. LEFT: SEM Image of single PET fiber (~20 μm diameter). RIGHT: SEM Image of PET fiber bundle (non-circular diameters)

Image 3.3 supports the previous images, clearly showing a collagen film deposited on the non-circular PET fibers. This image was taken on a site away from the bulk sample and close to the edge where the sample was cut from the rest of the graft, hence the damage on the uniformity of the collagen film.

Image 3.3. SEM image of PET fibers covered with collagen film (Woven, collagen-coated vascular graft).

After careful examination of the woven sample, images of the knitted sample were taken. Since it would be impossible to distinguish heparin at the magnifications achieved by the SEM used here, only one knitted sample was studied assuming both samples should show similar characteristics. Image 3.4 shows the surface morphology of the inside wall of a knitted PET vascular graft. The diameter of a fiber bundle is around

260 ± 17 μm ($n=4$), and the crimp width is about 920 ± 180 μm ($n=3$).

Image 3.4. SEM image of PET vascular graft, inside wall (Knitted)

Image 3.5 left and right show individual fibers. The left image reveals a fiber with a 15 μm diameter, once again, consistent with reasonable, expected PET fiber diameter [18]. The image on the right was not taken from a bulk sample, but from a collection of fibers pulled out of the edge of the graft. The collagen film has been overstretched, therefore it shrunk, due to the damaging of the sample.

Image 3.5. SEM Images of PET fibers used for knitted vascular graft.

Image 3.6 shows a cross-section of the graft wall, with a thickness of about 450 µm, sensibly similar to the expected 490 µm (as provided by manufacturer). The line added to the top right of the image denotes the interior wall of the graft. A denser, more visible layer of collagen film is observed closer to the red line in the bottom left of the image. This is expected from the manufacturing process (See Figure 1.4).

Image 3.6. SEM Image of PET vascular graft (Knitted, heparin bonded) cross-section, showing denser collagen sealant near the external wall of the graft.

There is a dramatic difference between the clearly defined topology of the interior wall shown in the previous images and the less oriented fibers on the exterior (not contacting blood flow) velour shown in Image 3.7.

Image 3.7. SEM images of PET vascular graft, external wall (knitted)

3.1.2. ATOMIC FORCE MICROSCOPY

AFM images of the vascular graft samples were taken to identify smaller features with better resolution than SEM, while eliminating the need to coat the surface with gold (which could potentially lead to contamination). The images not only revealed the surface topology of the grafts, but they also revealed the optimal sample preparation procedure (that with the least damaging to the sample) for the MFP experiments to follow. To do this, images were taken under different conditions to determine the effect of sample preparation, and scan angle. All AFM images were taken in air under contact mode.

In order to image the samples using the AFM, the crimps and undulations in the grafts had to be flattened out to allow for proper tip-surface engagement. Usual practice is to use a thin, commercial layer of adhesive to glue the sample onto the magnetic holder; however, the graft surfaces did not stayed attached to the holder using this

30

method. Presumably, the least damaging mounting technique would be one that does not involve gluing the sample to the holder. Therefore, a special sample holder (Figure 3.1) was designed to image a sample, held down by two spring clips.
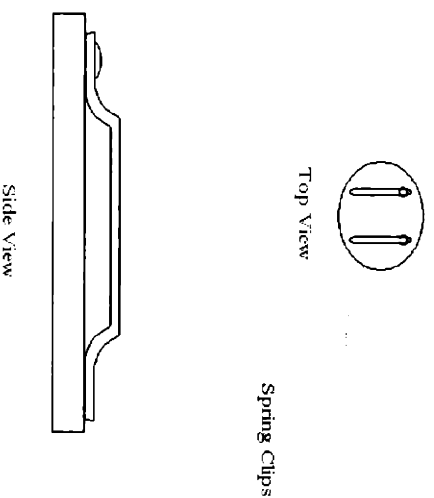

Top View

Spring Clips

Side View

Figure 3.1. Especially designed AFM sample holder.

Bare polyester fibers were imaged using this mounting technique. Image 3.8 shows the surface topology of the fibers at 5 and 10 μm scans. The surface of the fibers imaged is not smooth at the nanoscale, featuring an RMS roughness of 1.471 nm.

After thorough analysis of the unglued sample, images were taken from samples that were glued to the holder using Duco® cement (Devcon Consumer Products). In order to avoid surface contamination with cement, the adhesive layer was considerably thinner than the graft wall thickness. The glued sample was left to dry under a 5 kg weight to flatten the crimps. This method could potentially damage the surface of the samples, therefore a series of images were compared over a range of times in which the samples were left under the weight. Image 3.9 shows an image taken from a sample 5 minutes after being glued. The surface morphology of this fiber is similar to that of the previously studied sample.
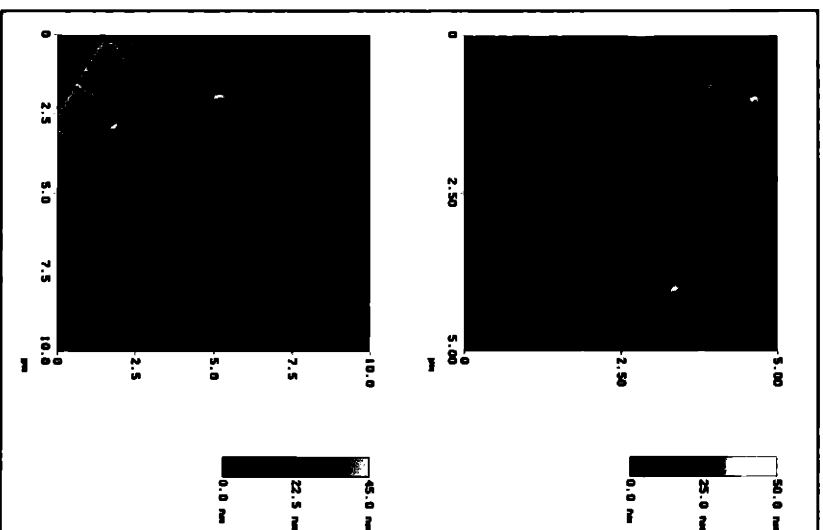
Image 3.8. AFM images of PET fiber surface. Sample was mounted on spring clip sample holder (not glued)
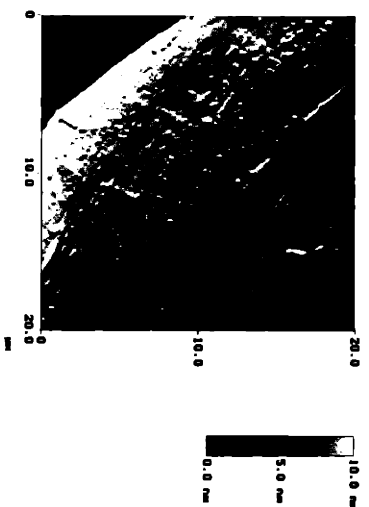

Image 3.9. AFM image of PET fiber surface. Sample was glued and left under 5 kg weight for 5 minutes.

Image 3.10 shows the surface of a fiber after being under the 5kg weight for one hour. The image on the top shows an apparent flattening of the surface; however, an

32

exact, direct comparison to the previous images cannot be made due to the possibility of different fibers having different degrees of roughness. RMS roughness of top image is 1.145 nm, which actually turns out to be more akin to the previous images than it visually appears. In order to understand if this change in surface morphology was universal to the fibers in the sample, a different fiber on that sample was imaged over a larger scan (bottom, Image 3.10). This image revealed a surface practically similar to the previous fibers studied. It should be noted that the image was taken with a large width to height ratio because the z-range of the piezo did not allow images to be taken once the probe tip lost contact with the surface during the scan, therefore a scan smaller than 20 μm (about the fiber diameter) in the direction normal to the longitudinal direction of the fiber must be used.
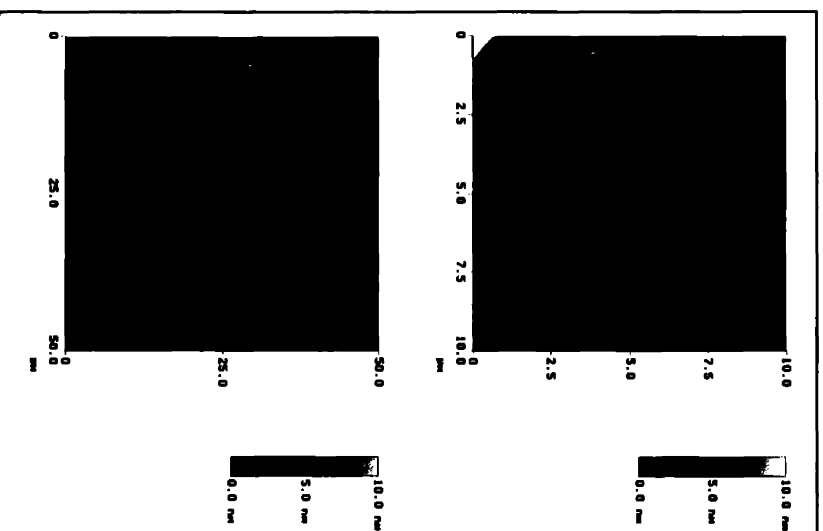
Image 3.10. AFM images of PET fiber surface. Sample was glued and left under 5 kg weight for 60 minutes.

One last sample was imaged after being compressed for one day under the 5 kg weight. Again, the surface morphology shown in Image 3.11 is comparable to the previously obtained images. RMS roughness of this sample is 1.321 nm. This series of images demonstrate that sample preparation technique (later used for MFP experiments) does not threaten the surface physical characteristics of the samples.
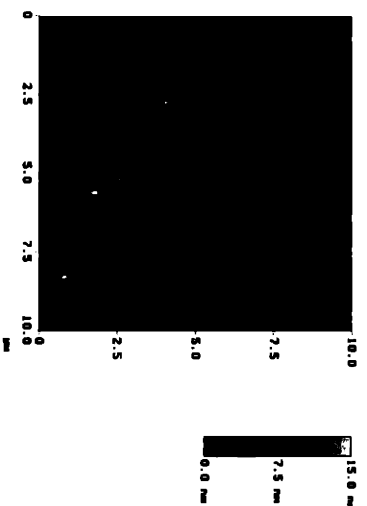
Image 3.11. AFM image of PET fiber surface. Sample was glued and left under 5 kg weight for 24 hours.

Surface-immobilized heparin is not distinguishable at the scale of the scans performed, therefore, only the collagen-coated fibers were imaged. Image 3.12 shows the difference in surface morphology for the collagen-coated PET caused by the collagen film. RMS roughness is 1.594 nm.
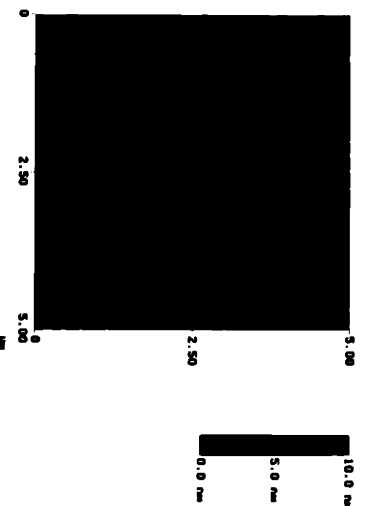
Image 3.12. AFM image of vascular graft (Knitted, collagen-coated) fiber. Sample was glued and left under 5 kg weight for one hour.

34

3.2. PROTEIN-GRAFT INTERACTIONS

3.2.1. MOLECULAR FORCE PROBE

The results for the MFP experiments are divided into two components: approach and retract data. Approach data is that collected as the cantilever probe tip is brought near the surface of the graft. This data collection, when averaged, reveals the attractive and repulsive forces experienced by the cantilever probe tip as the distance between the tip and the surface decreases. Retract data is collected as the cantilever probe tip is pulled away from the surface of the graft. The retract curves provide information about the forces and distances of adhesion observed as the distance between the cantilever probe tip and the graft surface is increased.

3.2.1.A. ON APPROACH

Force versus distance curves were measured at room temperature using a Thermomicroscopes microfabricated V-shaped Si_3N_4 cantilever probe tip ($k_c = 0.01$ N/m, cantilever length = 320 μm, resonant frequency = 850 Hz) against graft samples glued to a sample holder (as described in Section 2.1.2). All MFP experiments (except the ionic strength studies) were performed in 0.01 M Phosphate Buffer Solution (PBS). The Si_3N_4 (henceforth referred to as unfunctionalized) cantilever probe tip experiments were used as a 'control'.

Figure 3.2 shows the average force versus distance curves for the experiments described above. As expected, the heparin-bonded graft exhibits larger, longer range ($\sim$ 80 nm) repulsion than the rest of the curves, due to the presence of surface charges interacting with the probe tip. Both collagen-coated samples show a behavior similar to each other. Again, this is expected since both samples have a similar surface chemistry and surface charge. The bare polyester sample experiences the least amount of repulsion of all the samples, with a repulsion starting around 25 nm, similar to the collagen-coated samples.
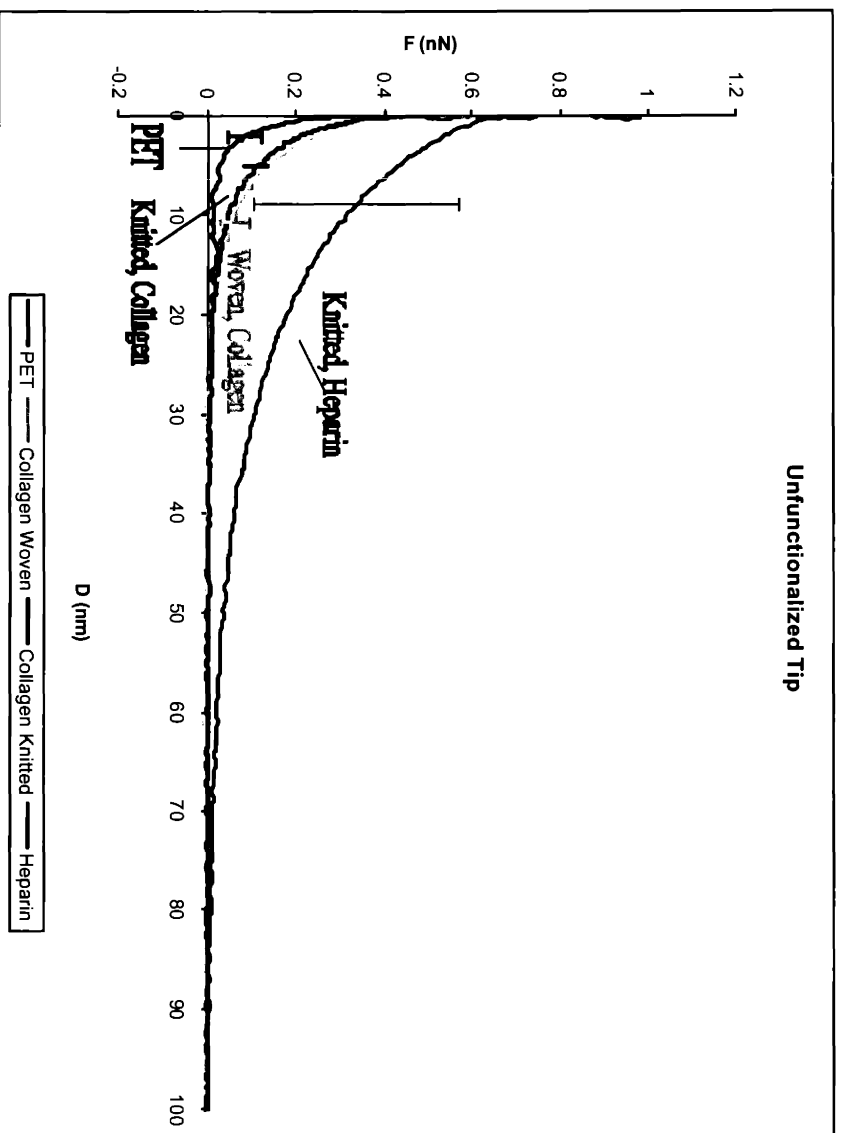

Figure 3.2. Average force vs. distance curves for an unfunctionalized Si_3N_4 cantilever probe tip against the different types of grafts.

In order to prove that the experiments being performed were actually measuring surface forces and not nanoindenting the sample, two approaches were taken. The first approach was to choose a cantilever with a low spring constant, so that the cantilever probe tip is much 'softer' than the surface. The second approach was to run a series of experiments with varying environmental conditions, expecting to see an effect on the behavior of the interactions. To do this, the ionic strength of the PBS solution was varied over 3 different orders of magnitude.

Figure 3.3 shows the effect of ionic strength on the magnitude and shape of the force versus distance curves. 0.01 and 1 M PBS show a long range repulsion starting around 60 nm. 0.15 M PBS experiments show a purely attractive interaction. These results prove the validity of the MFP experiments by exhibiting a change in the interactions as a function of environmental conditions.

Force as a function of IS
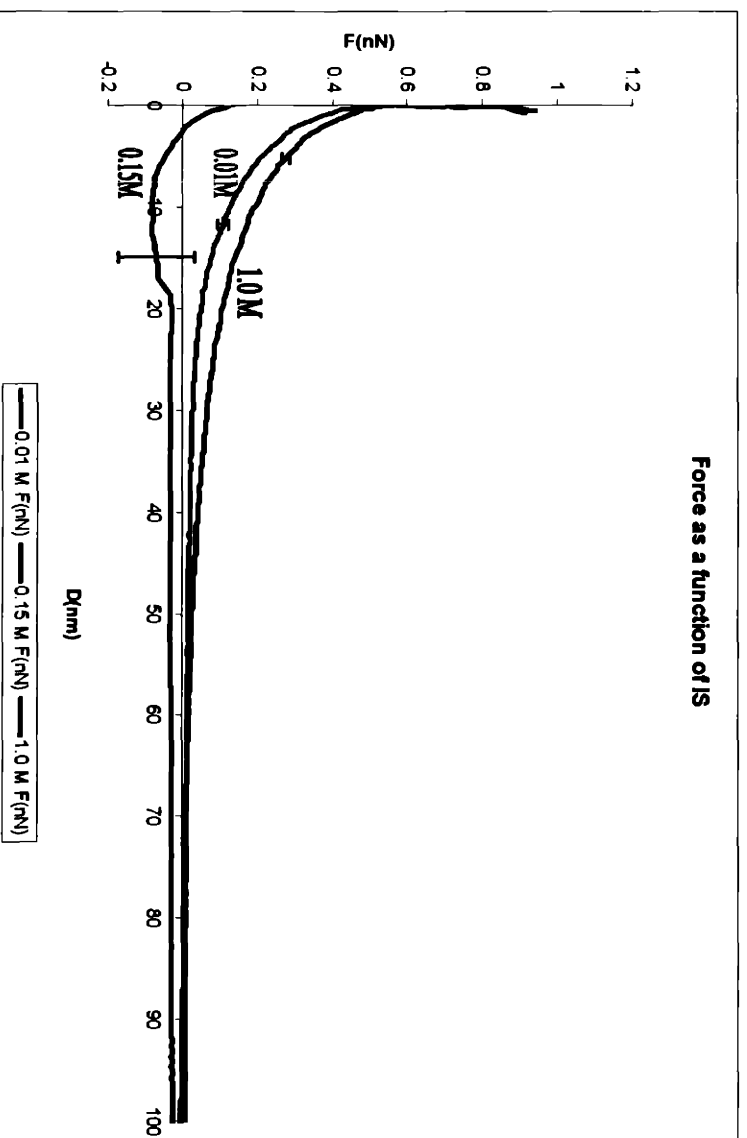
Figure 3.3. Force vs. distance curves under varied ionic strengths.

The cantilever probe tip was then functionalized with Human Serum Albumin (HSA) as explained in Section 2.3.1. Two hypotheses were proposed before starting the experiments: 1) surface chemistry determines the magnitude of the forces experienced on approach and 2) surface morphology plays a more significant role in these interactions. It should be noted that the bare PET graft is woven, as well as one of the collagen-coated grafts. The other two (collagen-coated and heparin) are knitted. Unmodified PET was expected to show the least repulsive character due to its significantly hydrophobic nature, since increased hydrophobicity of the surface of the material increases the strength of protein interactions [4]. Figure 3.4 shows that, indeed, PET experiences a repulsion smaller in magnitude than the rest of the grafts.

Figure 3.4. Average force versus distance curves between HSA-functionalized tip and different vascular graft samples.

38

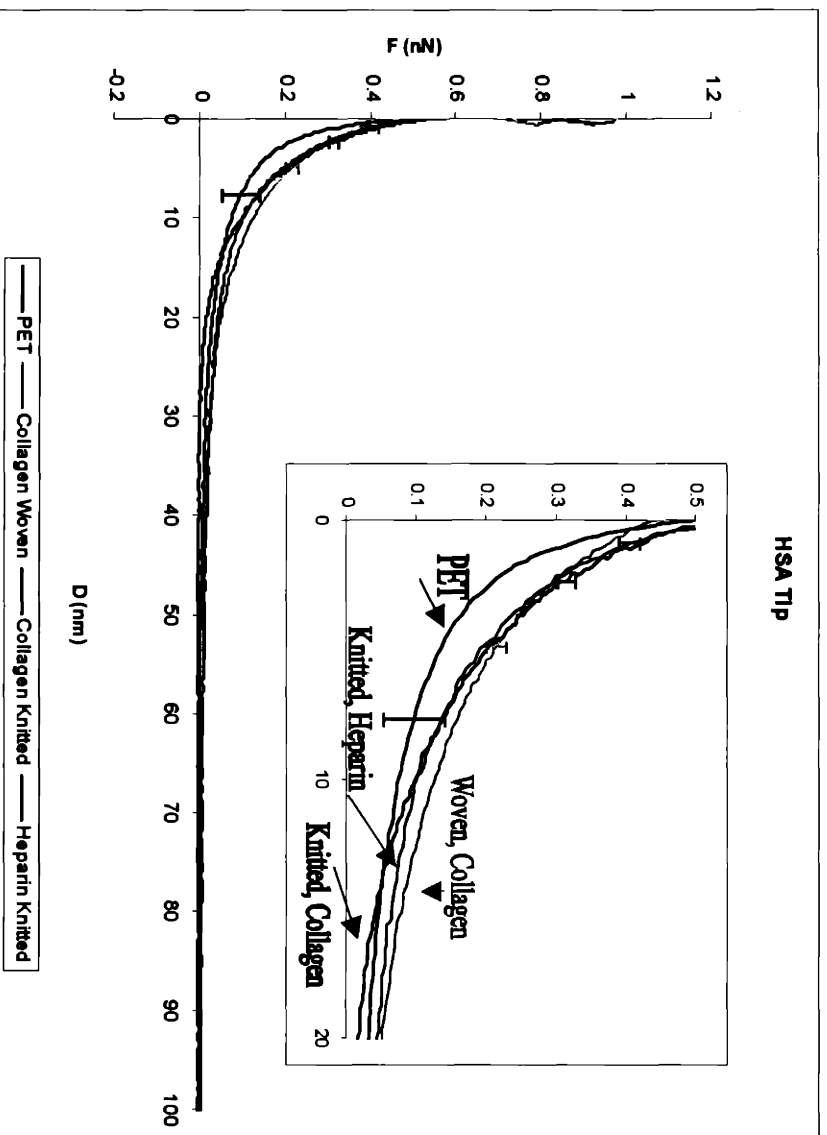All of the samples exhibit a long range repulsion starting at around 50 nm. Interestingly, the surface-modified PET samples all exhibit a very similar behavior on approach. A possible answer could be that heparin was inactivated during the surface attachment process. According to the literature, heparin bioactivity may be lost or inhibited because of degradation and/or blocking of binding sites from proteins [24]. However, these results could also be explained by the specific nature of heparin binding. As explained in Section 1.7, heparin binds specifically to antithrombin, not HSA. Therefore, heparin should not affect the force experienced between the probe tip and the surface, since HSA was actually interacting with only collagen in all three cases.

3.2.1.B. ON RETRACT

After the tip was brought in contact with the surfaces, it was retracted and the forces and distance observed were measured. Three different types of interactions were observed: 1) surface adhesion, 2) pulling, 3) surface adhesion followed by pulling (See section 2.3.2). Table 3.1 shows the percentage of occurrence for each graft.

Table 3.1. Frequencies of interactions between HSA-grafted probe tip and different graft samples

	PET	Collagen Woven	Collagen Knitted	Heparin Knitted
Pulling	8.7%	23.3%	4.3%	44.4%
Surface Adh	45.6%	34.5%	39.1%	9.7%
Both	42.7%	22.4%	56.5%	20.8%
Neither	2.9%	19.8%	0.0%	25.0%
Total # of curves	103	116	92	144

It should be noted that the heparin sample showed a significantly lower percentage of surface adhesion, with the majority of interactions being based on pulling.

This could be due to a potential change in the HSA adhesion mechanisms brought about by heparin's negatively-charged nature.
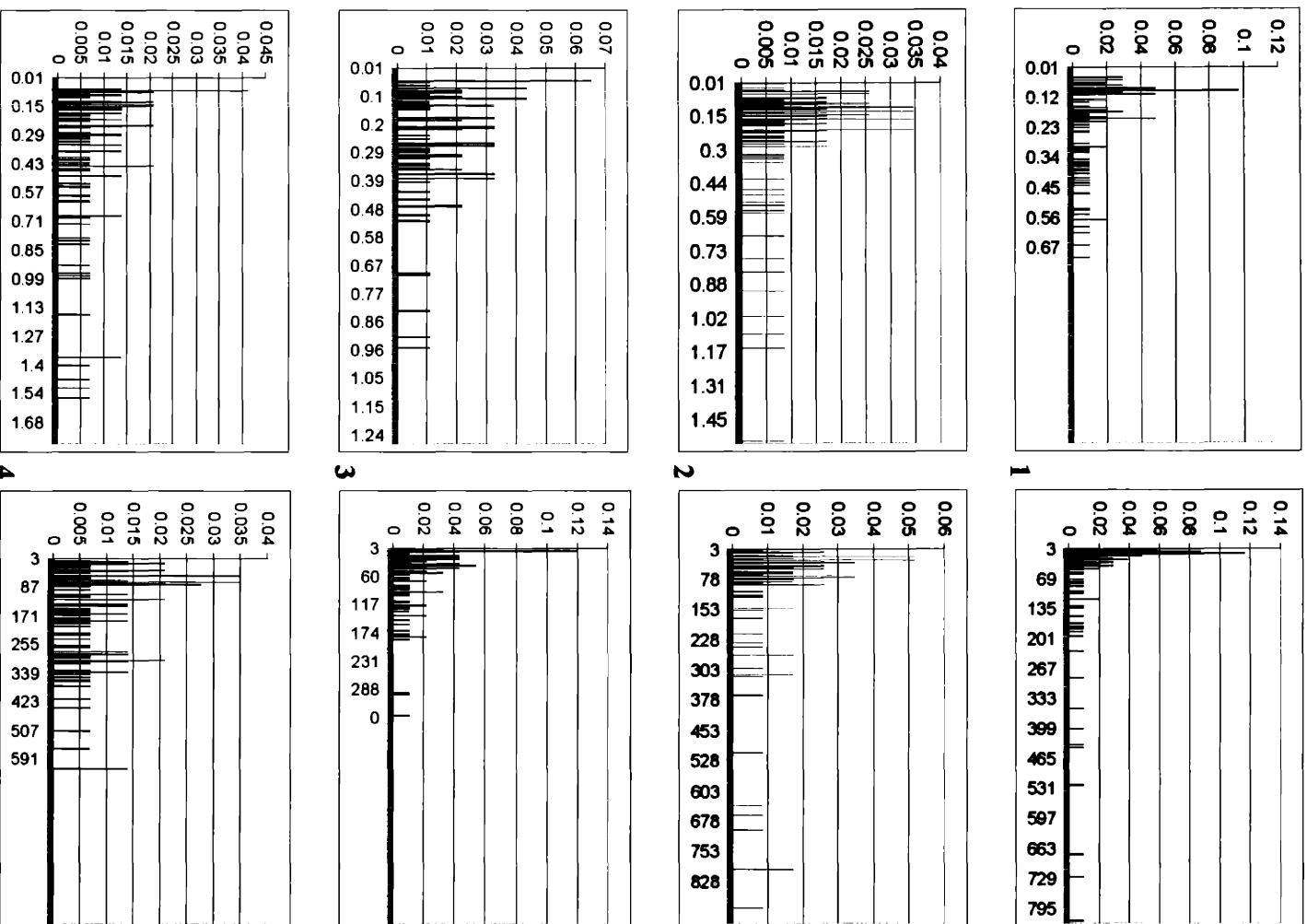

Figure 3.5 Probability histograms of different vascular grafts. *LEFT*: Force, *RIGHT*: Distance. 1: bare PET, 2: woven collagen-coated, 3: knitted collagen-coated, 4: knitted heparin-bonded.

40

Figure 3.5 shows the distribution of peaks in AFM force/distance experiments. The peak distance is corrected by 0.4548 nm.

Each force versus distance was analyzed individually, measuring the distance and force of pulling and/or adhesion. These forces and distances were averaged for each sample and displayed in Figure 3.6. $F_{adhesion}$ is the maximum attractive force observed on retraction for each distinct adhesion event. $D_{adhesion}$ is the distance corresponding to $F_{adhesion}$.

The most prominent feature of Figure 3.6 is found in the graph for $<F_{adhesion}>$ of extension (pulling). The numbers are considered extremely statistically different (as compared using student's t-test). It is important to note that the outlier averages correspond to the knitted samples. These results clearly show the dependence of the magnitude of the force on surface morphology of the graft. The rest of the graphs show a similar behavior for the different events.
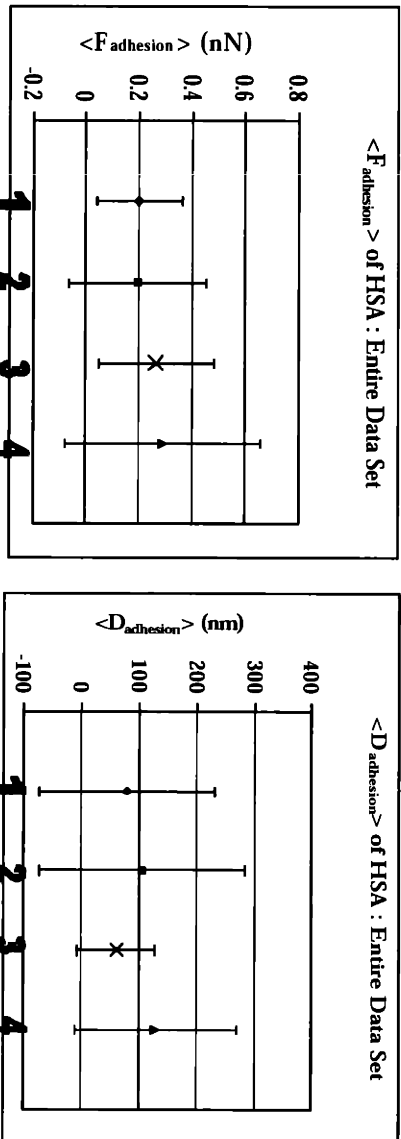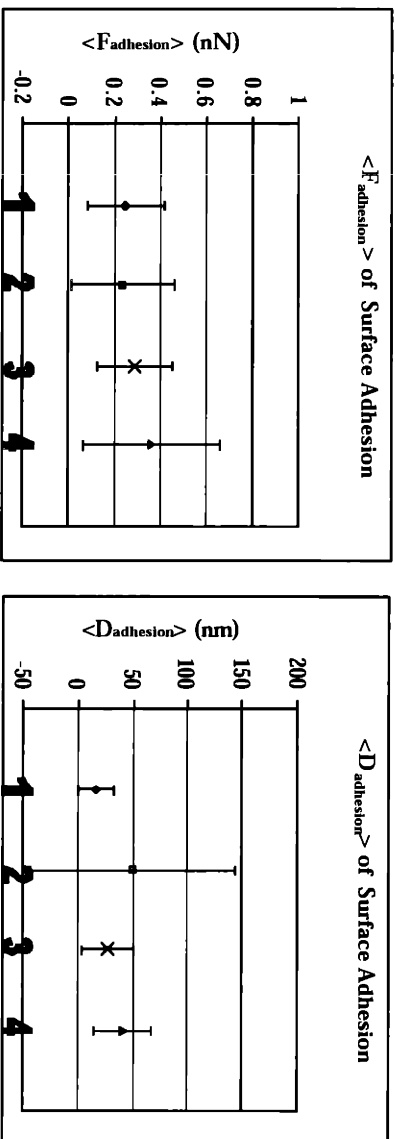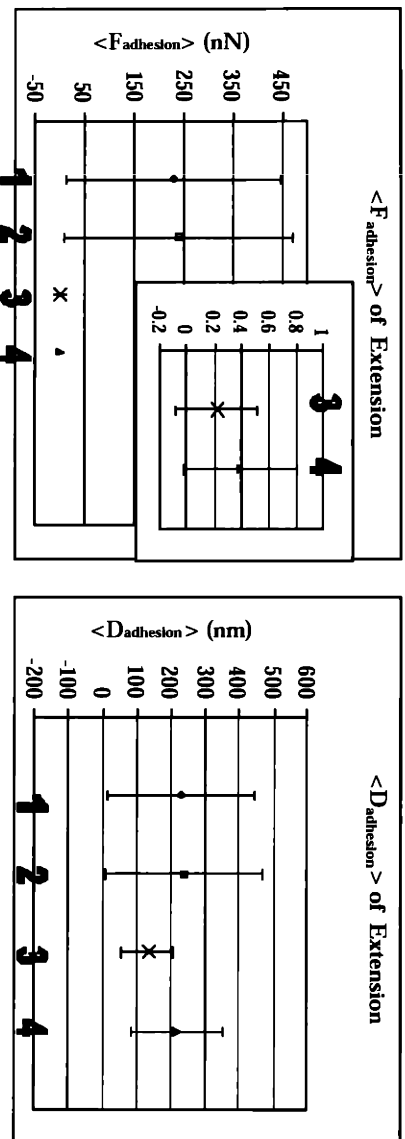
Figure 3.6 Average forces and distance of adhesion and pulling (extension) for HSA -grafted probe tip against the different grafts. 1:PET, 2: collagen-coated woven, 3: collagen-coated knitted, 4: heparin-bonded knitted.

42

CHAPTER 4
CONCLUSIONS AND RECOMMENDATIONS

Vascular grafts are an important field of study both in clinical medicine and in biomaterials science. Every year, vascular grafts save the lives of patients whose arteries have been damaged. A variety of macroscopic *in vivo* and *in vitro* studies have been performed for many years; still, a positively biocompatible synthetic vascular graft surface has not been achieved. Consequently, the goal of this thesis project was to combine standard characterization techniques with new advancements in nanotechnology in an effort to elucidate the molecular origins of the biological rejection response experienced by vascular grafts.

The objective of this project was to characterize and analyze the nanoscale surface properties of PET-based commercial vascular grafts. The study was performed in order to ascertain differences in biocompatibility due to surface coating and morphology. Scanning Electron Microscopy, Atomic Force Microscopy and High Resolution Force Spectroscopy techniques were used to characterize the surface of the samples as well as to measure the forces between these surfaces and blood plasma proteins. A thorough analysis of the grafts' physical properties provided the basis to draw conclusions relating the surface morphologies and their respective interactions with human serum albumin. SEM and AFM images displayed the characteristic topographies of the samples presenting an insight to their nano- and microscopic features.

Heparin's antithrombogenic properties have been shown to affect specific attractive interactions; however these properties are almost unsuccessful when it comes to

nonspecific interactions, which are in fact, important governing the activation of platelets during the first stage of the coagulation cascade.

The forces observed between HSA and all the surface-modified PET samples exhibit a very similar behavior on approach proving that HSA was actually interacting only with collagen in all three cases. Therefore, the surface morphology and the specific nature of heparin binding to antithrombin have little or no effect on the nonspecific interactions between proteins and surfaces on approach. Nevertheless, this behavior is not representative of either the interactions observed between other plasma proteins and biomaterials or the relationship of these interactions with the biomaterial surface morphology and chemistry.

A very different situation was observed once the protein was in contact with the surface. The bonded heparin seemed to change the attachment mechanism of HSA on the surface. While the collagen-coated samples exhibited mainly surface adhesion, the heparin-bonded graft was characterized by protein pulling. Surface morphology also played an important role on these interactions. The forces of protein pulling of the knitted samples were significantly different to those of the woven samples, regardless of surface chemistry.

The results here presented have the potential to prove that during the first stage of surface adhesion (adhesion of low molecular weight molecules, e.g. HSA) surface chemistry and morphology do not necessarily dictate the fate of the biomaterial in the human body. However, surface morphology and chemical modification of the PET fibers is certainly an important factor determining the mechanisms of protein adsorption.

A next set of experiments is recommended to support these results. The studies should include a comparison between these results and those obtained by similar experiments performed using antithrombin instead of human serum albumin. It would be interesting to also study the interactions between these proteins and a set of surfaces ranging from a flat to an extremely rough surface.

In order to engineer the next generation of synthetic vascular grafts, a thorough understanding of the nanoscale interactions between the biomaterial surface and blood plasma proteins is needed. The results presented here provide an insight into an alternative approach to future work in the design of vascular graft surfaces with better biocompatibility.

REFERENCES

[1]   D. F. Williams. "Definitions in biomaterials". *Proceedings of a Consensus Conference of the European Society for Biomaterials*. 1986

[2]   A. Halperin, D. C. Leckband. "From ship hulls to contact lenses: repression of protein adsorption and the puzzle of PEO". *Comptes Rendus de l'Académie des Sciences - Series IV - Physics*, **9**, *1171-1178*, 2000

[3]   E. Laemmel, J. Penhoat, R. Warocquier-Clerout, M. Sigot-Luizard. "Heparin immobilized on proteins usable for arterial prosthesis coating: Growth inhibition of smooth-muscle cells". *J Biomed Mater Res*, **39**, 446-452, 1998

[4]   D. Falkenback, F. Lundberg, E. Ribbe, A. Ljungh. "Exposure of plasma proteins on Dacron and ePTFE vascular graft material in a perfusion model". *Eur J Vasc Endovasc Surg*, **19**, 468-475, 2000

[5]   T. Chandy, G. S. Das, R. F. Wilson, G. Rao. "Use of plasma glow for surface-engineering biomolecules to enhance blood compatibility of Dacron and PTFE vascular prosthesis". *Biomaterials*, **21**, 699-712, 2000

[6]   J. A. Chinn, J. A. Sauter, R. E. Phillips, W. J. Kao, J. M. Anderson, S. R. Hanson, T. R. Ashton. "Blood and tissue compatibility of modified polyester: Thrombosis, inflammation, and healing". *J Biomed Mater Res*, **39**, 130-140, 1998

[7]   Intervascular, Inc. "InterGard Heparin: A proven alternative to PTFE grafts for femoro-popliteal reconstruction". Educational Service

[8]   M. D. Phaneuf, D. J. Dempsey, M. J. Bide, W. C. Quist, F. W. LoGerfo. "Coating of Dacron vascular grafts with an ionic polyurethane: a novel sealant with protein binding properties". *Biomaterials*, **22**, 463-469, 2001.

[9]   I. Goodman, J. A. Rhys. *Polyesters*. American Elsevier Pub. Co.: New York, NY, 1965

[10]   J. Scheirs, T. E. Long. *Modern Polyesters: Chemistry and Technology of Polyesters and Copolyesters*. John Wiley & Sons, Ltd: England, 2003

[11] R. J. Young, P. A. Lovell. *Introduction to Polymers*, Second Edition. Chapman & Hall: New York, NY, 1991

[12] S. Dumitriu. *Polymeric Biomaterials*, Second Edition. Marcel Dekker, Inc: New York, NY, 2002

[13] R. D. Pascoe, B. O'Connell. "Flame treatment for the selective wetting and separation of PVC and PET". *Waste Management*, **23**, 845-850, 2003.

[14] J. B. Park, R. S. Lakes. *Biomaterials: An introduction*. Plenum Press: New York, NY, 1992

[15] T. Nezu, F. M. Winnik. "Interaction of water-soluble collagen with poly(acrylic acid)". *Biomaterials*, **21**, 415-419, 2000

[16] Y. Sun, Z. Luo, A. Fertala, K. An. "Direct quantification of the flexibility of type I collagen monomer". *Biochemical and Biophysical Research Communications*, **295**, 382-386, 2002

[17] M. J. B. Wissink, R. Beernink, J. S. Pieper, A. A. Poot, G. H. M. Engbers, T. Beugeling, W. G. van Aken, J. Feijen. "Immobilization of heparin to EDC/NHS-crosslinked collagen. Characterization and in vitro evaluation". *Biomaterials*, **22**,151-163, 2001

[18] W. J. van der Giessen, H. M. van Beusekom, R. Larsson, P. W. Serruys. "Heparin-Coated Coronary Stents". *Current Interventional Cardiology Reports*, **1**, 234-240, 1999

[19] S. Dumitriu. *Polymeric Biomaterials*. Marcel Dekker, Inc: New York, NY, 1993

[20] P. C. Begovac, R. C. Thomson, J. L. Fisher, A. Hughson, A. Gallhagen. "Improvements in GORE-TEX® Vascular Graft Performance by Carmeda® BioActive Surface Heparin Immobilization". *Eur J Vasc Endovasc Surg*, **25**, 432-437, 2003

[21] M. J. B. Wissink, R. Beernink, A. A. Poot, G. H. M. Engbers, T. Beugeling, W. G. van Aken, J. Feijen. "Improved endothelialization of vascular grafts by local release of growth factor from heparinized collagen matrices". *Journal of Controlled Release*, **64**, 103-114, 2000.

[22]   M. O. Dayhoff. *Atlas of Protein Sequence and Structure*, National Biomedical Foundation: Washington DC, 1972.

[23]   M. A. Rixman, D. Dean, C. E. Macias, C. Ortiz. "Nanoscale Intermolecular Interactions Between Human Serum Albumin and Alkanethiol Self-Assembling Monolayers". *Langmuir*, **19**, 6202-6218, 2003

[24]   C. Nojiri, T. Kido, T. Sugiyama, K. Heriuchi, T. Kijima, K. Hagiwara, E. Kuribayashi, A. Nogawa, K. Ogiwara, T. Akutsu. "Can heparin immobilized surfaces maintain nonthrombogenic activity during in vivo long-term implantation?" *Am Soc Artif Intern Organs J*, **17**, 6-9, 1971

[25]   B. D. Ratner, A. S. Hoffman, F. J. Schoen, J. E. Lemons. *Biomaterials Science*. Academic Press: San Diego, CA, 1996